

1.5- μm -band wavelength conversion based on difference-frequency generation in LiNbO_3 waveguides with integrated coupling structures

M. H. Chou, J. Hauden,* M. A. Arbore, and M. M. Fejer

E. L. Ginzton Laboratory, Stanford University, Stanford, California 94305-4085

Received January 28, 1998

We report wavelength conversion within the 1.5- μm telecommunications band based on difference-frequency generation in periodically poled lithium niobate waveguides with integrated coupling structures. A conversion efficiency of -7 dB and a normalized efficiency of 260%/W are demonstrated. Static tests show that the conversion bandwidth is 72 nm and the conversion efficiency is constant over the 20-dB range of input powers tested. © 1998 Optical Society of America

OCIS codes: 190.2620, 190.4390, 060.4510.

Wavelength conversion is a useful function for wavelength-division multiplexed networks.¹ Among numerous wavelength-conversion technologies, difference-frequency generation (DFG) is attractive because it offers strict transparency to amplitude, frequency, and phase information; excess-noise-free and chirp-reversed signal output; an extremely high input dynamic range; and a bit rate limited only by the extremely wide parametric conversion bandwidth.² DFG-based devices are also able to convert multiple wavelengths simultaneously. The expansion of the system's bit rate will not degrade the performance of DFG-based devices. Recently, an architecture for a wavelength-interchanging cross connect using DFG-based wavelength converters was proposed.³ That architecture, exploiting the unique properties of DFG-based wavelength converters, has been shown to be scalable and rearrangeably nonblocking.

Wavelength conversion by use of DFG in AlGaAs (Ref. 4) and annealed proton-exchanged LiNbO_3 (Refs. 5 and 6) waveguides has been demonstrated. The results of Ref. 4 showed a -17 -dB conversion efficiency with a 90-nm conversion bandwidth for 65 mW of launched pump power; dynamic tests performed at 2.5 Gbits/s showed a clear eye diagram. The reported results suffered from low conversion efficiencies because of high propagation losses (in AlGaAs) or limited homogeneous interaction lengths (in LiNbO_3). Another critical issue with guided-wave DFG is the launching of short-wavelength (typically half of the signal wavelength) pump light into the fundamental mode of the multimoded (at the pump) waveguide required for confining the signal. In this Letter we address the device optimization and solve the mode launching problem by using integrated mode coupling structures, resulting in a conversion efficiency of -7 dB and a normalized efficiency of 260%/W.

DFG is based on three-wave mixing using large second-order nonlinearities. A strong pump at wavelength λ_p mixes with a (usually weak) signal at wavelength λ_s to generate an output (idler) at wavelength λ_{out} , where $1/\lambda_p = 1/\lambda_s + 1/\lambda_{\text{out}}$. In the limit of pump nondepletion, this DFG process can be described

by the relation⁷

$$E_{\text{out}}^* = iE_s \sinh(\Gamma E_p), \quad (1)$$

where E_{out}^* is the complex conjugate of the output electric field, E_s is the input signal field, E_p is the pump field, and Γ is a constant that is proportional to the interaction length in the device, the overlap of the interacting modal fields, and the material nonlinearity $\chi^{(2)}$. The above parametric process permits operation at arbitrarily low input signal powers, preserves signal phase information, and reverses signal chirp. The power conversion efficiency scales linearly with the pump power in the limit of low conversion efficiency:

$$\begin{aligned} P_{\text{out}}/P_s &= \sinh^2(\eta_{\text{norm}} P_p)^2 \\ &\approx \eta_{\text{norm}} P_p \quad (\text{for } \eta_{\text{norm}} P_p < 1), \end{aligned} \quad (2)$$

where P_{out} is the converted output power, P_s is the input signal power, P_p is the pump power, and η_{norm} is the normalized efficiency (expressed in units of W^{-1} rather than in the %/W form commonly used in the DFG literature). The normalized efficiency is related to conversion efficiency $\eta(\text{dB}) \equiv 10 \log(P_{\text{out}}/P_s)$ by

$$\begin{aligned} \eta &= 10 \log[\sinh^2(\eta_{\text{norm}} P_p)^{1/2}] \\ &\approx 10 \log(\eta_{\text{norm}} P_p) \quad (\text{for } \eta_{\text{norm}} P_p < 1). \end{aligned} \quad (3)$$

As we discuss subsequently, relation (3) is valid in the limit of the pump nondepletion.

In DFG, one or both of the signal and output fields must be at a wavelength significantly longer than that of the pump. A waveguide that supports any modes at the longest wavelength is necessarily multimoded for the pump. Because of waveguide dispersion, only one of the pump modes (generally the fundamental mode) will contribute to the phase-matched DFG process. It is difficult to couple the pump radiation exclusively into the fundamental mode of such a multimoded structure, resulting in poor performance owing to unused pump power in high-order modes. It has been shown that fundamental mode excitation of a multimoded waveguide can be achieved

by use of an adiabatic taper implemented with periodically segmented waveguides (PSW's).⁸ One period, of length Λ , of a PSW consists of a segment of length l indiffused with a dopant to produce an index change Δn , separated by undoped regions of length $\Lambda - l$. PSW's can be approximated by an equivalent waveguide in which the effective refractive-index step is taken to be $\Delta n_{\text{eff}} = \Gamma \Delta n$, where the duty cycle is $\Gamma = l/\Lambda$. Hence an appropriate taper in the duty cycle can be used to implement a desired taper in the confinement. The waveguide is defined in a single lithography step, providing a practical device fabrication method.

Off-degenerate (signal wavelength λ_s not much different from pump wavelength λ_p) DFG using adiabatic tapers has been demonstrated⁹; in this case a single taper was used for coupling both the pump and the signal into the conversion region. To implement near-degenerate ($\lambda_s \sim 2\lambda_p$) DFG we developed a more sophisticated waveguide structure, which includes a mode filter, an adiabatic taper, a directional coupler, and a wavelength converter, as shown in Fig. 1. Both the mode filter and the adiabatic taper are implemented with PSW's. In this configuration the pump is coupled into a single-mode waveguide, which acts as a mode filter and can be optimized for efficient fiber pig-tailing. A subsequent adiabatic taper efficiently couples the pump radiation into the fundamental mode of the difference-frequency mixer. The signal is routed into the wavelength-conversion region with a directional coupler, which bypasses the pump filter region and does not significantly perturb the pump mode. This integrated structure permits efficient and stable mode launching of both inputs.

We optimized the device for wavelength conversion within the 1.5- μm band, basing the design on previously developed models of the linear and nonlinear properties of annealed proton-exchanged waveguides^{10,11} in LiNbO_3 . The beam propagation method was used to model the adiabatic taper and the directional coupler. We chose a proton-exchange depth of 0.55 μm and a width of 5.5 μm and annealed to a depth of 1.6 μm . The 2.5-mm-long mode filter had a segmentation duty cycle of 35%, the 5-mm-long taper had duty cycles that varied smoothly from 35% to 100%, the 1.5-mm-long directional coupler had a 10- μm center-to-center separation, and the DFG region was 30 mm long. The theoretical internal normalized efficiency of this device, neglecting propagation losses, is $\sim 800\%/W$, with a 3-dB bandwidth of ~ 60 nm. For an ideal device, 0-dB conversion efficiency should be obtained for 100-mW pump power. Taking into account waveguide propagation losses (typically ~ 0.4 dB/cm), 0-dB conversion efficiency should be possible with a pump power of 140 mW.

Samples were fabricated upon a 7.62-cm-diameter wafer of LiNbO_3 periodically poled with a 14.5- μm period by the electric-field poling method.^{12,13} Waveguides were formed by proton exchange through a SiO_2 mask in pure benzoic acid for 3.6 h at 177 $^\circ\text{C}$ and annealed at 333 $^\circ\text{C}$ for 9 h. First we characterized the samples by measuring the second-harmonic-generation (SHG) wavelength tuning curve, because the near-degenerate DFG has the same normalized efficiency

as SHG. The device had a peak normalized efficiency of 270%/W and a FWHM SHG bandwidth of 0.36 nm, which is wider than the 0.3 nm theoretically predicted for a 30-mm device. We attribute this discrepancy to waveguide inhomogeneities, consistent with the somewhat distorted shape of the SHG tuning curve. We estimate from the area under the tuning curve that, in the absence of nonuniformities, the peak normalized efficiency would have been $\sim 500\%/W$.¹⁴

Static wavelength-conversion tests were performed with a cw Ti:sapphire laser at 784 nm for the pump and a cw tunable erbium-doped-fiber laser for the signal. These two beams were free-space launched into two different waveguides by an objective lens and combined into the wavelength converter by the integrated directional coupler, as discussed above. The pump light exiting the waveguide was imaged onto a CCD camera, with which it was seen that the fundamental mode of the waveguide was excited. With 67-mW pump power exiting the waveguide (after correction for the Fresnel loss of the uncoated end face), we observed a stable conversion efficiency of -7 dB, implying a normalized efficiency of 260%/W (assuming 0.4 dB/cm propagation losses). Figure 2 shows a measured optical spectrum on a log scale for a signal at 1539 nm and its converted output, which has been shifted by 58 nm to 1597 nm.

DFG-based devices have the same conversion efficiency over a wide signal power range; the saturation of conversion comes from the depletion of pump power. The conversion efficiency reduction $\Delta\eta$ (dB) that is due to the pump power depletion can be expressed in terms of Jacobi elliptic functions.¹⁵ For $\eta P_p < 1$ and $P_s < P_p$, $\Delta\eta$ can be approximated by

$$\Delta\eta \approx 10 \log(1 + \eta_{\text{norm}} P_s). \quad (4)$$

For an ideal device with a normalized efficiency of 800%/W the conversion efficiency will be reduced by 0.035 dB for a 0-dBm input signal or by 0.34 dB for 10 dBm. For the device with a normalized efficiency of 260%/W the reduction will be smaller than the resolution in this experiment. We performed wavelength conversion by varying the input signal power (~ -20 to -40 dBm); the conversion efficiency is constant over the 20-dB range tested.

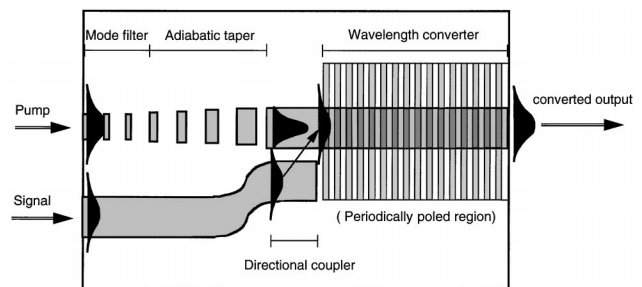


Fig. 1. Schematic of the integrated waveguide structure. A mode filter and an adiabatic taper, both implemented with periodically segmented waveguides, couple the pump into the fundamental mode of a waveguide. A directional coupler routes the signal into the single-mode wavelength-conversion region.

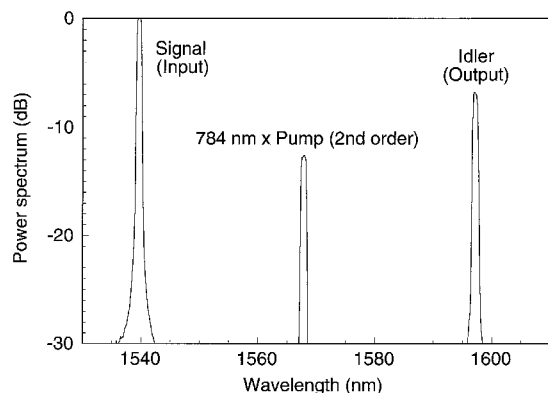


Fig. 2. Measured optical spectrum on a log scale of a signal at 1539 nm and its converted output, which has been shifted 58 nm to 1597 nm. The central peak at 1568 nm is the second-order spectrometer response to the pump wavelength of 784 nm. The conversion efficiency for the output pump power of 67 mW is -7 dB, corresponding to a normalized efficiency of $\sim 260\%/W$.

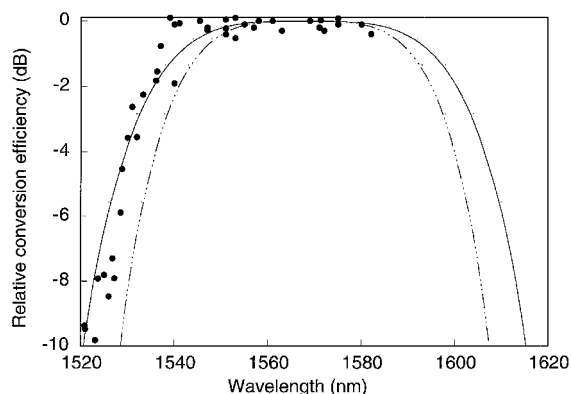


Fig. 3. Relative conversion efficiency as a function of input signal wavelength: filled circles, measured results; solid curve, a fit based on measured SHG results; dashed curve, the theoretical calculation for an ideal 30-mm-long device.

By tuning the input signal wavelength, we measured the conversion bandwidth, as shown in Fig. 3. This device shows a 3-dB signal bandwidth of 72 nm, larger than the 60-nm signal bandwidth for an ideal 30-mm-long device but consistent with the broader-than-ideal tuning curve measured for SHG. Using two $1.5\text{-}\mu\text{m}$ lasers, we performed wavelength conversion simultaneously for two input channels; the same conversion efficiency was observed for both channels.

Photorefractive effects were observed at room temperature, manifested as shifts in the phase-matching curve by as much as 7 nm. These shifts were eliminated by operation at 90°C and were substantially reduced in a sample annealed in an O_2 atmosphere. We expect to facilitate operation at temperatures closer to room temperature by further reducing photorefractive effects through improved device fabrication, such as by eliminating process steps that subject the sample to elevated temperature in reducing atmospheres.

In summary, we have demonstrated efficient wavelength conversion within the $1.5\text{-}\mu\text{m}$ band by using DFG in periodically poled LiNbO_3 waveguides

with integrated coupling structures. A static conversion efficiency of -7 dB, a constant conversion efficiency for the 20-dB range of signal powers tested, a conversion bandwidth of 72 nm, and simultaneous conversion of two channels have been shown. With further improvements in the device fabrication process and design, 0-dB conversion efficiency should be possible with a diode laser pump. Future research will involve dynamic measurements and investigations of polarization-insensitive designs. This integrated structure can also be useful for bidirectional wavelength conversion between the 1.3 and $1.5\text{-}\mu\text{m}$ bands, gated mixing for time-division multiplexed networks, and spectroscopic experiments that require sources of infrared radiation where diode lasers are unavailable.

This research is supported by the Defense Advanced Research Projects Agency and by the Joint Services Electronics Program. J. Hauden thanks the International Department of the French Research Ministry. We also thank Crystal Technology for its generous donation of LiNbO_3 substrates and G. D. Miller for fruitful discussions.

*Present address, Laboratoire d'Optique P. M. Duffieux, Université de Franche-Comte, 25030 Besançon Cedex, France.

References

1. C. A. Brackett, *IEEE J. Sel. Areas Commun.* **8**, 948 (1990).
2. S. J. B. Yoo, *J. Lightwave Technol.* **14**, 955 (1996).
3. X. N. Antoniadis, K. Bala, S. J. B. Yoo, and G. Ellinas, *IEEE Photon. Technol. Lett.* **8**, 10 (1996).
4. S. J. B. Yoo, R. Bhat, C. Caneau, and M. A. Koza, in *Conference on Lasers and Electro-Optics*, Vol. 11 of 1997 OSA Technical Digest Series (Optical Society of America, Washington, D.C., 1997), paper CMF3.
5. C. Q. Xu, H. Okayama, and M. Kawahara, *Appl. Phys. Lett.* **63**, 3559 (1993).
6. M. L. Bortz, D. Serkland, M. M. Fejer, and S. J. B. Yoo, in *Conference on Lasers and Electro-Optics*, Vol. 8 of 1994 OSA Technical Digest Series (Optical Society of America, Washington, D.C., 1994), paper CTHD6.
7. R. L. Byer, in *Nonlinear Optics*, P. G. Harper and B. S. Wherrett, eds. (Academic, San Diego, Calif., 1997), p. 85.
8. M. H. Chou, M. A. Arbore, and M. M. Fejer, *Opt. Lett.* **21**, 794 (1996).
9. M. A. Arbore, M. H. Chou, and M. M. Fejer, in *Conference on Lasers and Electro-Optics*, Vol. 9 of 1996 OSA Technical Digest Series (Optical Society of America, Washington, D.C., 1996), paper JTUE2.
10. M. L. Bortz and M. M. Fejer, *Opt. Lett.* **16**, 1844 (1991).
11. M. L. Bortz, L. A. Eyres, and M. M. Fejer, *Appl. Phys. Lett.* **62**, 2012 (1993).
12. L. E. Myers, R. C. Eckardt, M. M. Fejer, R. L. Byer, W. R. Bosenberg, and J. W. Pierce, *J. Opt. Soc. Am. B* **12**, 2102 (1995).
13. G. D. Miller, R. G. Batchko, M. M. Fejer, and R. L. Byer, *Proc. SPIE* **2700**, 34 (1996).
14. M. L. Bortz, S. J. Field, M. M. Fejer, W. D. Nam, R. G. Waarts, and D. F. Welch, *IEEE J. Quantum Electron.* **30**, 2953 (1994).
15. J. A. Armstrong, N. Bloembergen, J. Ducuing, and P. S. Pershan, *Phys. Rev.* **127**, 1918 (1962).